

Cutoff dependence of the thrust peak position in the dipole shower

Robin Baumeister and Stefan Weinzierl

*PRISMA Cluster of Excellence, Institut für Physik,
Johannes Gutenberg-Universität Mainz,
D - 55099 Mainz, Germany*

Abstract

We analyse the dependence of the peak position of the thrust distribution on the cutoff value in the Nagy-Soper dipole shower. We compare the outcome of the parton shower simulations to a relation of the dependence from an analytic computation, derived within soft-collinear effective theory. We show that the result of the parton shower simulations and the analytic computation are in good agreement.

1 Introduction

Parton showers are widely used in event generators like Pythia [1, 2], Herwig [3, 4] or Sherpa [5–7]. There are several variants of parton showers available (angular ordered showers [8, 9], dipole showers [10–25], antenna showers [26–28] etc.). Common to all parton showers is the dependence on two important parameters: The coupling, usually specified by the value $\alpha_s(m_Z)$ and the cutoff scale Q_0 . While the physical meaning of the former parameter is immediately clear – it describes the strength of the interaction –, the dependence on the latter parameter has received recently more attention [29]. This has been triggered to some extent by the desire to understand top quark mass measurements [30–35]. In the extraction of the top mass from experimental measurements theory sneaks in through the use of the template method or the matrix element method. For example, within the template method one generates first by Monte Carlo a sample of events for various values of m_{MC} and then determines the best fit to the experimental data. The Monte Carlo mass m_{MC} is only implicitly defined through the program code of the event generator. We would like to relate the Monte Carlo mass m_{MC} to a theoretically well-defined mass. In order to avoid renormalon ambiguities the theory mass should be a short-distance mass. The MSR-mass [36, 37] is a good candidate. The MSR-mass depends on two scales, a UV-scale μ and an IR-scale R , such that

$$m_{\text{MSR}}(R=0) = m_{\text{pole}}, \quad m_{\text{MSR}}(R=\bar{m}) = \bar{m}. \quad (1)$$

Here, \bar{m} denotes the $\overline{\text{MS}}$ -mass. The MSR-mass is a short-distance mass for $R \gg \Lambda_{\text{QCD}}$. The definition of the MSR-mass can be understood in the context of effective theories, which separates the various relevant scales (the centre-of-mass energy Q , the top mass m_t , the top width Γ_t and Λ_{QCD}). It can be shown that physics at scales in the range of $[\Gamma_t, m_t]$ affect the position of the peak of the reconstructed top mass distribution, and these effects depend on m_t . Physics at scales in the range of $[\Lambda_{\text{QCD}}, \Gamma_t]$ affect the peak position as well, but these effects are described by soft physics and are independent of m_t . Thus $R \approx \Gamma_t$ is a natural choice for the infrared scale. It is a numerical coincidence that the shower cutoff is typically of the order of Γ_t . Furthermore the shower cutoff provides naturally an infrared scale for the parton shower. This implies that the Monte Carlo mass m_{MC} is closely related to the MSR-mass with the IR-scale R being of the order of the shower cutoff Q_0 .

In an idealised perfect event simulator an observable like the peak position of the reconstructed top mass distribution should be independent of a technical parameter like the shower cutoff. The explicit dependence on the shower cutoff will be compensated by a change in the modelling of soft physics and by a change of the IR-scale R in the top mass definition. This dependence is in principle calculable analytically, and keeping the modelling of soft physics and the IR-scale R fixed one obtains a prediction how the peak position of the reconstructed top mass distribution in simulated events depends on the shower cutoff.

In order to understand the situation better, it is helpful to consider a related problem: The dependence of the peak position of the thrust distribution in electron-positron annihilation on the shower cutoff [38]. This quantity has the advantage that analytic results are available for the dependence on the shower cutoff (contrary to the case discussed above). The analytic results may be derived within soft-collinear effective theory or alternatively within the coherent branching

formalism [3, 8, 39, 40]. In a recent publication [29] a study has been performed which compares the analytic results with numerical results from an angular ordered shower as implemented in Herwig. Clearly, the coherent branching formalism is closely tied to an angular ordered shower. However, the analytic results in [29] have been derived with the assumption that the shower cutoff provides a restriction on the transverse momentum of the emitted particles. Furthermore, the second derivation in [29] based on soft-collinear effective theory uses just the condition on the transverse momentum and is not tied to any particular shower algorithm. We thus expect these results to hold for any shower algorithm whose shower evolution variable reduces in the singular limit to p_\perp . This is a hypothesis which can be tested and verified by a dedicated study: This is the content of the present paper. We show that the theoretical prediction is not only valid for angular ordered parton showers but holds for Nagy-Soper dipole showers (with p_\perp as evolution variable) as well. By a Nagy-Soper dipole shower we mean a shower algorithm as proposed in refs. [16, 17]. As an analytic treatment of the Nagy-Soper dipole shower is out of reach, we do this by comparing the theoretical prediction with numerical results from shower simulations. Comparing the results of [29] with our results we observe that the dipole shower agrees slightly better with the theoretical predictions.

This paper is organised as follows: In the next section we review the analytic computations for the cutoff dependence and give the essential relation. In section 3 we present our analysis and results using the dipole shower. Finally, our conclusions are contained in section 4.

2 Analytic results

We study the observable “one minus thrust” τ in electron-positron annihilation, defined by

$$\tau = 1 - T. \tag{2}$$

The thrust is defined by

$$T = \frac{1}{Q} \max_{\vec{n}} \sum_j |\vec{p}_j \cdot \vec{n}|, \tag{3}$$

where Q denotes the centre-of-mass energy, \vec{p}_j denotes the three-momentum of particle j and the sum runs over all particles in the final state. The thrust variable maximises the total longitudinal momentum along the unit vector \vec{n} . We will study this observable in massless QCD, where the leading order Born process is $e^+e^- \rightarrow Z/\gamma \rightarrow \bar{q}q$, with massless quarks q . We also study this observable in top-pair production in electron-positron annihilation, where the leading order Born process is $e^+e^- \rightarrow Z/\gamma \rightarrow \bar{t}t$. In the former case (massless QCD) the definition (3) agrees with the conventional definition of thrust [41, 42]

$$T = \frac{\max_{\vec{n}} \sum_j |\vec{p}_j \cdot \vec{n}|}{\sum_j |\vec{p}_j|}, \tag{4}$$

in the latter case (massive quark production) with the definition used in [43,44]. For the analysis, the peak position of the τ distribution, τ_{peak} , is considered. It is strongly affected by configurations containing two jets that are back-to-back. These contributions arise from the leading order production of a quark-antiquark pair. For massless quark production, the region of the peak is close to $\tau = 0$. This location is shifted to positive values due to non-perturbative effects. The size of this shift is of order $O(\Lambda/Q)$, where $\Lambda \approx 1$ GeV [45–48]. For massive quark production, the peak is located around $\tau = 2m^2/Q^2$ [29]. The thrust distribution makes a reasonable choice for the study of the cutoff dependence of a parton shower because there exist analytic calculations for the thrust distribution based on factorisation, that the parton shower outcome can be compared to.

The hadronic thrust distribution in the peak region is given by [48–50]

$$\frac{d\sigma}{d\tau}(\tau, Q) = \int_0^{\tau Q} d\mu \frac{d\sigma_{\text{sing}}}{d\tau} \left(\tau - \frac{\mu}{Q}, Q \right) S_{\text{mod}}(\mu), \quad (5)$$

where $d\sigma_{\text{sing}}/d\tau$ contains the resummed singular partonic QCD corrections (i.e. terms corresponding to $\alpha_s^n \delta(\tau)$ and $\alpha_s^n [\ln^k(\tau)/\tau]_+$) and the soft model shape function S_{mod} describes soft-gluon non-perturbative effects. In our numerical studies we substitute $d\sigma_{\text{sing}}/d\tau(\tau, Q)$ by $d\sigma_{\text{shower}}/d\tau(\tau, Q, Q_0)$. The latter is obtained from a simulation with hard matrix elements at the scale Q and shower evolution from the hard scale Q to the shower cutoff scale Q_0 .

2.1 The massless case

We start with the case of massless QCD. The leading order Born process is $e^+e^- \rightarrow Z/\gamma \rightarrow \bar{q}q$, with massless quarks q . We take the same soft model shape function S_{mod} as in [29]

$$S_{\text{mod}}(\mu) = \frac{128}{3} \frac{\mu^3}{\Lambda_m^4} \exp\left(-\frac{4\mu}{\Lambda_m}\right), \quad (6)$$

where Λ_m is a smearing parameter, that is varied between 1 and 3 GeV. The soft model shape function causes a smearing of the partonic thrust distribution that shifts the position of the peak to the positive direction. We denote by $\tau_{\text{peak}}(Q_0)$ the peak position of the hadronic thrust distribution, where $d\sigma_{\text{sing}}/d\tau$ has been substituted by $d\sigma_{\text{shower}}/d\tau$. We are interested in the peak position as a function of the shower cutoff Q_0 , while all other parameters are kept fixed. From soft-collinear effective theory (or the coherent branching formalism) one predicts [29]

$$\tau_{\text{peak}}(Q_0) = \tau_{\text{peak}}(Q'_0) - \frac{16}{Q} \int_{Q'_0}^{Q_0} dR \frac{\alpha_s(R) C_F}{4\pi}. \quad (7)$$

Here, $\tau_{\text{peak}}(Q'_0)$ is the value of the peak position at some reference scale Q'_0 .

For physical meaningful results a change in the shower cutoff from Q'_0 to Q_0 should be accompanied by a modification of the soft model shape function S_{mod} according to

$$\frac{d\sigma}{d\tau}(\tau, Q, Q_0) = \int_0^{\tau Q} d\mu \frac{d\sigma_{\text{shower}}}{d\tau} \left(\tau - \frac{\mu}{Q}, Q, Q'_0 \right) S_{\text{mod}}(\mu + \Delta_{\text{soft}}(Q_0) - \Delta_{\text{soft}}(Q'_0)). \quad (8)$$

Δ_{soft} is called the gap function [51]. The gap can be calculated perturbatively. The infrared insensitive difference between the gap function at the two scales yields to leading order

$$\Delta_{\text{soft}}(Q_0) - \Delta_{\text{soft}}(Q'_0) = 16 \int_{Q'_0}^{Q_0} dR \frac{\alpha_s(R) C_F}{4\pi}. \quad (9)$$

The primary purpose of this paper is to verify that a dipole shower behaves as predicted by factorisation and soft-collinear effective theory. Thus we keep the soft model shape function fixed and verify eq. (7).

On the other hand, if we correspondingly modify the soft model shape function according to eq. (8), the peak position of the thrust distribution should be independent of the cutoff Q_0 . We also verify this relation.

2.2 The massive case

We now consider the massive case. The leading order Born process is $e^+e^- \rightarrow Z/\gamma \rightarrow \bar{t}t$. We denote by m_{MC} the Monte Carlo mass used in the hard matrix element and in the parton shower. We assume the hierarchy

$$Q_0 \ll m_{\text{MC}} \ll Q. \quad (10)$$

As in ref. [29] we modify the parameter Λ_m entering the soft model shape function according to

$$\Lambda_m \rightarrow \Lambda_m + 4 \frac{m_{\text{MC}} \Gamma_{\text{MC}}}{Q} \quad (11)$$

to account for some additional smearing due to the top quark width $\Gamma_{\text{MC}} = 1.5\text{GeV}$. Again we study the peak position $\tau_{\text{peak}}(Q_0)$ as a function of the shower cutoff Q_0 , while keeping all other quantities fixed. In the massive case, eq. (7) generalises to

$$\tau_{\text{peak}}(Q_0) = \tau_{\text{peak}}(Q'_0) - \frac{1}{Q} \left[16 - 8\pi \frac{m_{\text{MC}}}{Q} \right] C_F \int_{Q'_0}^{Q_0} dR \frac{\alpha_s(R)}{4\pi}. \quad (12)$$

Note that in this case the shift in the peak position is less pronounced due to the alternating sign in the square bracket. For physical meaningful results a change in the shower cutoff should be

accompanied by a modification of the soft model shape function as above and a redefinition of the Monte Carlo mass m_{MC} :

$$m_{\text{MC}}(Q_0) - m_{\text{MC}}(Q'_0) = -2\pi C_F \int_{Q'_0}^{Q_0} dR \frac{\alpha_s(R)}{4\pi}. \quad (13)$$

As before, we are in this paper primarily concerned to verify that a dipole shower behaves as predicted by factorisation and soft-collinear effective theory. Thus we keep the soft model shape function and the Monte Carlo mass fixed and verify eq. (12).

3 Dipole shower results

In this section we simulate events with the Nagy-Soper dipole shower algorithm [16, 17]. For the dipole shower algorithm we use the implementation of ref. [18]. We first study the massless case, where we verify eq. (7) and eq. (8). We then proceed to the massive case and verify eq. (12).

As most showers, the implementation of ref. [18] is of leading-logarithmic accuracy (LL), meaning that the shower correctly reproduces all leading-logarithmic terms (in the leading-colour approximation). Leading-log parton showers include some, but not all next-to-leading logarithms (NLL). The construction of NLL parton showers is a topic of current research [23–25]. Eqs. (7), (8) and (12) give the leading terms for the dependence on the cutoff parameter Q_0 . The dependence on the cutoff is approximately proportional to $(Q_0 - Q'_0)$ and shows up in LL and NLL terms. Thus NLL accuracy is a sufficient, but not necessary condition for a parton shower to follow the predicted cutoff dependence from SCET.

3.1 The massless case

In the massless case we consider the hard process $e^+e^- \rightarrow Z/\gamma \rightarrow \bar{q}q$ with massless quarks q at the centre-of-mass energy Q , followed by the dipole parton shower with cutoff scale Q_0 . For the strong coupling we use the leading-order formula

$$\alpha_s(\mu) = \frac{4\pi}{\beta_0 \ln \frac{\mu^2}{\Lambda^2}}, \quad \beta_0 = 11 - \frac{2}{3}N_f \quad (14)$$

with $\Lambda_5 = 88$ MeV corresponding to $\alpha_s(m_Z) = 0.118$. For the centre-of-mass energy we consider $Q = m_Z$ and $Q = 300$ GeV. For our analysis, we generate 10^7 events for each cutoff scale Q_0 between 0.6 GeV and 2.0 GeV in steps of 0.2 GeV. The histograms are created with a bin size of $\Delta\tau = 10^{-3}$. Note that this procedure gives the partonic thrust distribution generated by the dipole parton shower algorithm. To make it comparable to the analytic results we convolve the partonic thrust distribution with the soft model shape function as in (5). For that purpose we convolve the partonic thrust distribution $d\sigma_{\text{shower}}/d\tau$ with the S_{mod} of (6) using the discretised representation of the convolution integral.

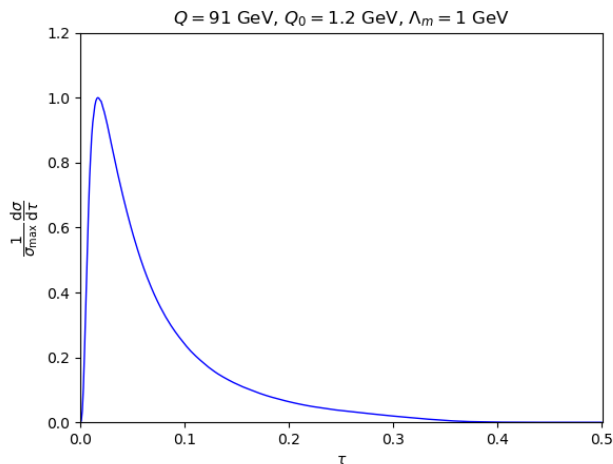


Figure 1: Thrust distribution for the centre-of-mass energy $Q = m_Z$, with the cutoff value $Q_0 = 1.2 \text{ GeV}$ and the smearing parameter of the soft model shape function $\Lambda_m = 1 \text{ GeV}$. The distribution is normalized such that its peak value is one.

As an example, we show the convolved partonic thrust distribution with the cutoff $Q_0 = 1.2 \text{ GeV}$ and the smearing parameter $\Lambda_m = 1 \text{ GeV}$ for $Q = m_Z$ in fig. 1. Note that we normalize all distributions in this paper such that the peak values are one.

Let us now address the question, how the position of the peak changes as a function of the cutoff Q_0 , while keeping all other quantities fixed. In particular we keep the soft model shape function fixed.

Fig. 2 shows the thrust distribution for the smearing parameters $\Lambda_m = 1 \text{ GeV}$ (left column) and $\Lambda_m = 3 \text{ GeV}$ (right column) with $Q = m_Z$ (upper panel) and $Q = 300 \text{ GeV}$ (lower panel), each with three different values for the shower cut. The red solid line represents a cut of $Q_0 = 1 \text{ GeV}$. The green dashed line and the blue dotted line stand for the cutoff values $Q_0 = 1.6 \text{ GeV}$ and $Q_0 = 2 \text{ GeV}$, respectively. Already from the plots for the three different cutoff values we can recognize the tendency that is implied by the analytic prediction (7): The value of the peak position decreases for larger cutoff values.

To obtain a more quantitative analysis of the peak position's dependence on the cutoff, we fit a quadratic function to the thrust distribution in the peak region and extract the maximum. This procedure ensures that the statistical uncertainties in the determination of the peak position are so small that we desist from specifying any systematic or statistical errors in our results. The results from this analysis are shown in fig. 3. The plot of the peak position against the cutoff Q_0 from the analytic formula is obtained by solving the integral in (7) numerically. As reference value we take the peak position from the parton shower simulation at $Q'_0 = 1.2 \text{ GeV}$.

Fig. 3 illustrates the position of the peak τ_{peak} as a function of the cutoff Q_0 for four different combinations of Q and Λ_m . The two upper figures correspond to $Q = m_Z$ with $\Lambda_m = 1 \text{ GeV}$ (left) and $\Lambda_m = 3 \text{ GeV}$ (right), while the two lower figures depict the Q_0 dependence for $Q = 300 \text{ GeV}$ with $\Lambda_m = 1 \text{ GeV}$ (left) and $\Lambda_m = 3 \text{ GeV}$ (right). The blue solid line shows the analytic

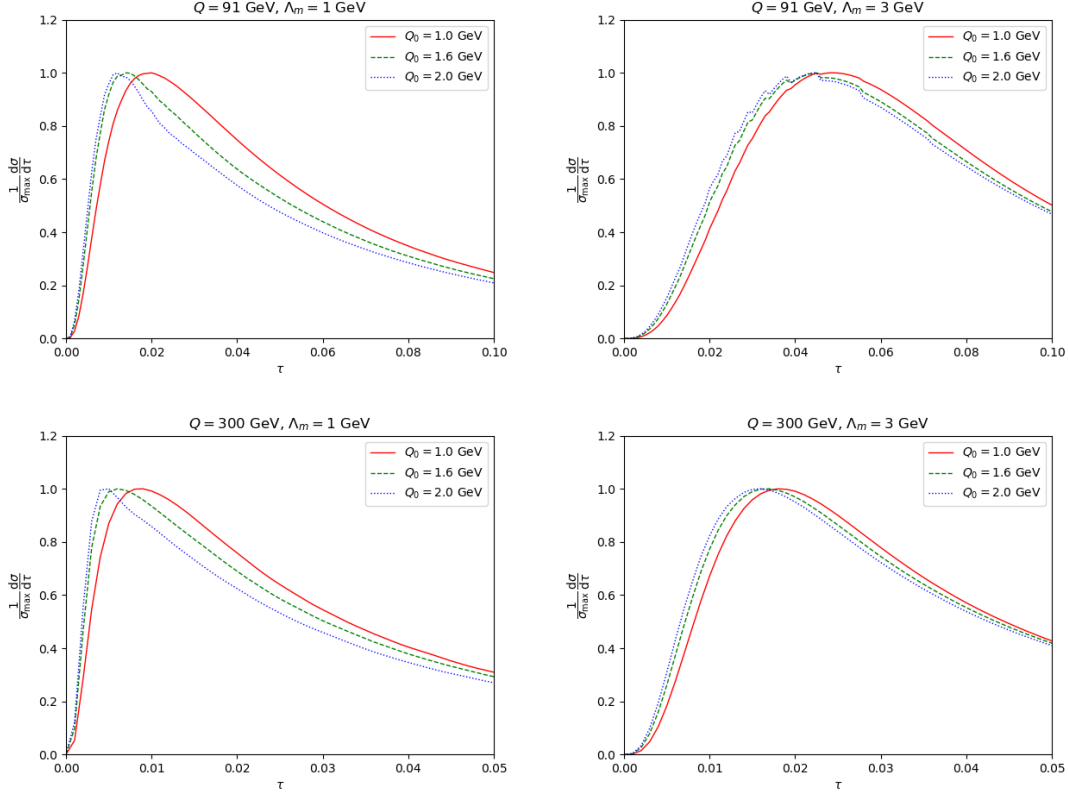


Figure 2: Plots of the thrust distribution from the dipole shower for the smearing parameters $\Lambda_m = 1$ GeV (left) and $\Lambda_m = 3$ GeV (right) for the a centre-of-mass energies $Q = m_Z$ (upper) and $Q = 300$ GeV (lower). Each figure shows the distribution for cutoff values of $Q_0 = 1$ GeV (red solid line), $Q_0 = 1.6$ GeV (green dashed line), and $Q_0 = 2$ GeV (blue dotted line), respectively.

relation (7). The centres of the red squares are the data points obtained from the parton shower simulations.

From fig. 3 we deduce a good agreement between the analytical prediction and the parton shower simulations from the dipole shower formalism. Hence, our results coincide with the findings of [29].

In the plots above we verified that the shower behaves as expected. For physical observables a change in the shower cutoff should be accompanied by a modification of the soft model shape function as in eq. (8).

In fig. 4 we show the position of the peak of the thrust distribution as a function of the shower cutoff Q_0 , where we modify the soft model shape function according to eq. (8). We expect that the leading terms cancel in the combination and indeed fig. 4 shows that the result is independent of the cutoff Q_0 . In fig. 4 the results for $Q = m_Z$ and $\Lambda_m = 1$ GeV are displayed.

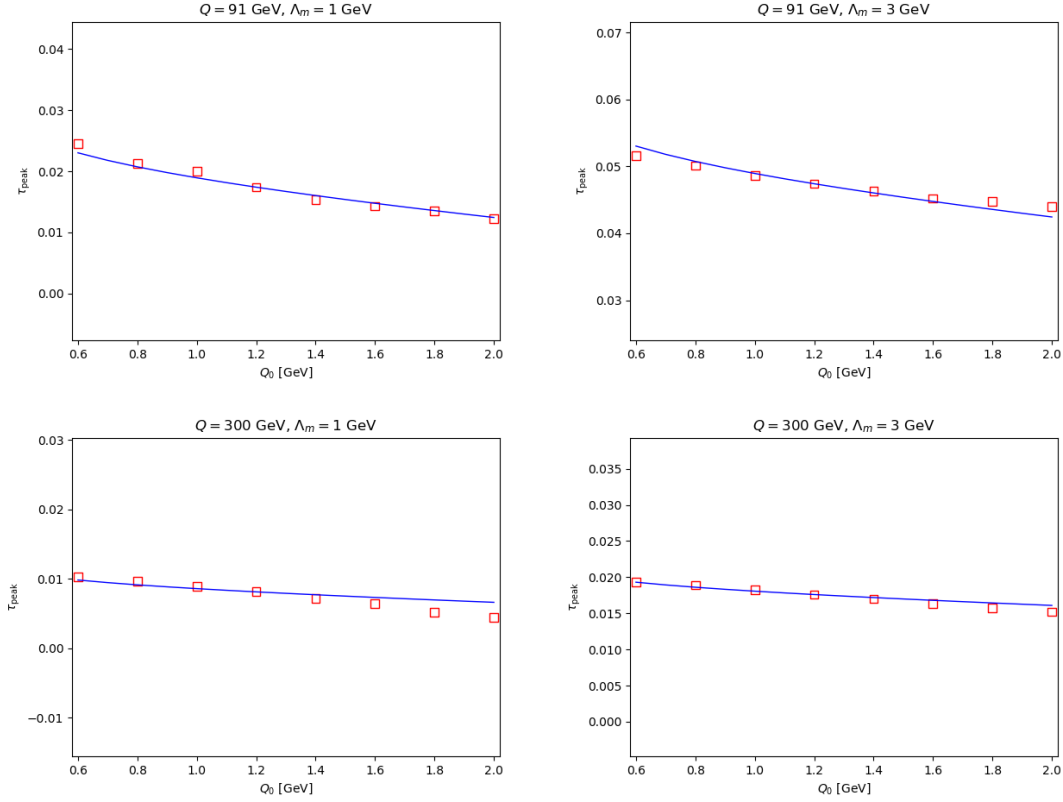


Figure 3: Position of the peak of the thrust distribution as a function of the shower cutoff Q_0 . Displayed are the plots for $Q = m_Z$ with $\Lambda_m = 1$ GeV (upper left) and $\Lambda_m = 3$ GeV (upper right) as well as $Q = 300$ GeV with $\Lambda_m = 1$ GeV (lower left) and $\Lambda_m = 3$ GeV (lower right). The blue solid line depicts the result of the analytical computation while the red squares represent the data points from the parton shower simulation.

3.2 The massive case

We now turn to the massive case. We consider the hard process $e^+e^- \rightarrow Z/\gamma \rightarrow \bar{t}t$ at the centre-of-mass energy Q , followed by the dipole parton shower with cutoff scale Q_0 . The analytic results are derived under the assumption of the hierarchy

$$Q_0 \ll m_{\text{MC}} \ll Q. \quad (15)$$

Thus we consider $m_{\text{MC}} = 173$ GeV and $Q = 1000$ GeV. The original implementation of [18] uses in the massive case the evolution variable

$$t = \ln \frac{-p_{\perp}^2 + (1-z)^2 m_i^2 + z^2 m_j^2}{Q^2}, \quad (16)$$

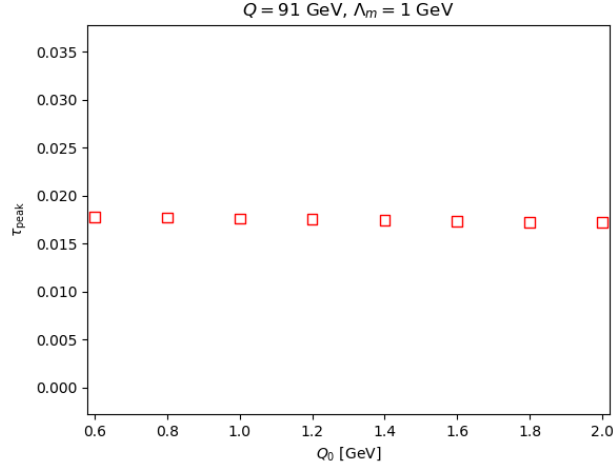


Figure 4: Position of the peak of the thrust distribution as a function of the shower cutoff Q_0 when the soft model shape function is modified accordingly. Displayed is a plot for $Q = m_Z$ with $\Lambda_m = 1 \text{ GeV}$.

as suggested by [3, 46]. m_i and m_j are the masses of the emitter and the emitted particle after the splitting. For this publication we changed the evolution variable to

$$t = \ln \frac{-p_{\perp}^2}{Q^2}. \quad (17)$$

Thus all numerical results in this paper are obtained by using the transverse momentum as the shower evolution variable. The plots in the massive case are based on 10^5 events for each cutoff scale Q_0 . The cutoff scale is again varied between 0.6 GeV and 2.0 GeV in steps of 0.2 GeV. We study again the peak position as a function of the cutoff Q_0 , while keeping all other quantities fixed. In particular we keep the soft model shape function and the Monte Carlo mass fixed. From eq. (12) we expect the shift in the peak position to be less pronounced, mainly due to the larger centre-of-mass energy, which enters as a $1/Q$ -prefactor but also due to the alternating sign in the factor $16 - 8\pi m_{\text{MC}}/Q$.

In the soft model shape function we use

$$\Lambda_m = \Lambda_{m,0} + 4 \frac{m_{\text{MC}} \Gamma_{\text{MC}}}{Q}, \quad (18)$$

as indicated by eq. (11).

Fig. 5 shows our results. The centre-of-mass energy is $Q = 1000 \text{ GeV}$. For the top quark we take $m_{\text{MC}} = 173 \text{ GeV}$ and $\Gamma_{\text{MC}} = 1.5 \text{ GeV}$. The left figure corresponds to $\Lambda_{m,0} = 1 \text{ GeV}$ while the right figure depicts $\Lambda_{m,0} = 3 \text{ GeV}$. The blue solid line shows the analytic relation (12). The centres of the red squares are the data points obtained from the parton shower simulations. We observe a good agreement between the analytical prediction and the numerical shower result.

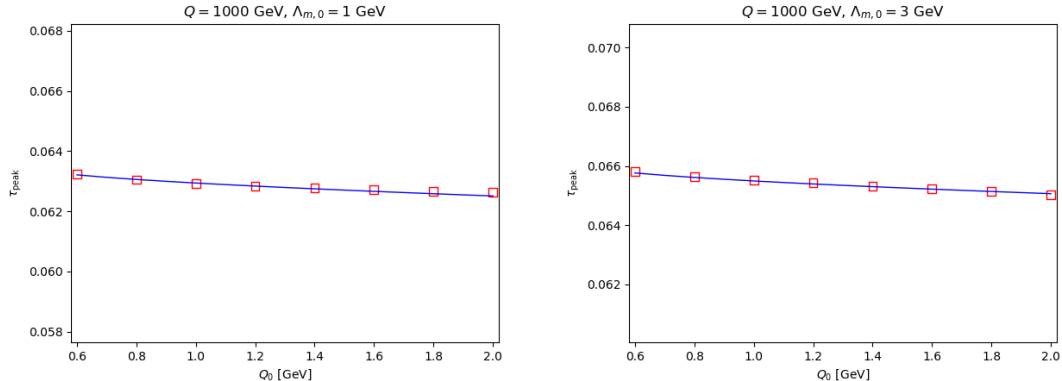


Figure 5: Position of the peak of the thrust distribution as a function of the shower cutoff Q_0 for $e^+e^- \rightarrow \bar{t}t$. The centre-of-mass energy is $Q = 1000\text{ GeV}$. Displayed are the plots for $\Lambda_{m,0} = 1\text{ GeV}$ (left) and $\Lambda_{m,0} = 3\text{ GeV}$ (right). The blue solid line depicts the result of the analytical computation while the red squares represent the data points from the parton shower simulation.

4 Conclusions

In this paper we analysed the cutoff dependence of the thrust peak position using an implementation of the Nagy-Soper dipole parton shower. We did this for the massless case and the massive case. We showed that the results of the numerical shower simulation agree with the analytic relations found in [29]. The analytic relations have been derived within soft-collinear effective theory (or alternatively the coherent branching formalism). This is an important verification. It shows that the results of [29] are not restricted to an angular ordered shower, but apply to a dipole shower with transverse momentum as evolution variable as well. We expect the results to hold for any parton shower whose shower evolution variable reduces in the singular limit to p_\perp . In particular we expect our results to apply to the default shower of the Sherpa event generator [19], as this shower is an independent implementation of the same shower algorithm we are using.

More generally, given an observable, a parton shower and an effective theory describing adequately the physics at the scales of the parton shower we expect that an observable like the shift of the peak position can systematically be calculated in the effective theory for the given parton shower algorithm.

Turning to phenomenology, the results of this paper improve our understanding of the Monte Carlo mass, which in turn is important for the determination of the top quark mass.

Acknowledgements

We thank Simon Plätzer for useful comments and discussions.

This work has been supported through the BMBF project “Precision calculations for collider and Higgs physics at the LHC” (Project ID 05H18UMCA1).

References

- [1] T. Sjöstrand and P. Z. Skands, *Eur. Phys. J.* **C39**, 129 (2005), hep-ph/0408302.
- [2] T. Sjöstrand *et al.*, *Comput. Phys. Commun.* **191**, 159 (2015), arXiv:1410.3012.
- [3] S. Gieseke, P. Stephens, and B. Webber, *JHEP* **12**, 045 (2003), hep-ph/0310083.
- [4] J. Bellm *et al.*, *Eur. Phys. J.* **C76**, 196 (2016), arXiv:1512.01178.
- [5] F. Krauss, R. Kuhn, and G. Soff, *JHEP* **02**, 044 (2002), hep-ph/0109036.
- [6] F. Krauss, A. Schälicke, and G. Soff, *Comput. Phys. Commun.* **174**, 876 (2006), hep-ph/0503087.
- [7] T. Gleisberg *et al.*, *JHEP* **02**, 007 (2009), arXiv:0811.4622.
- [8] G. Marchesini and B. R. Webber, *Nucl. Phys.* **B238**, 1 (1984).
- [9] B. R. Webber, *Nucl. Phys.* **B238**, 492 (1984).
- [10] G. Gustafson, *Phys. Lett.* **B175**, 453 (1986).
- [11] G. Gustafson and U. Pettersson, *Nucl. Phys.* **B306**, 746 (1988).
- [12] B. Andersson, G. Gustafson, and L. Lönnblad, *Nucl. Phys.* **B339**, 393 (1990).
- [13] B. Andersson, G. Gustafson, L. Lönnblad, and U. Pettersson, *Z. Phys.* **C43**, 625 (1989).
- [14] L. Lönnblad, *Comput. Phys. Commun.* **71**, 15 (1992).
- [15] L. Lönnblad, *JHEP* **05**, 046 (2002), hep-ph/0112284.
- [16] Z. Nagy and D. E. Soper, *JHEP* **10**, 024 (2005), hep-ph/0503053.
- [17] Z. Nagy and D. E. Soper, A New parton shower algorithm: Shower evolution, matching at leading and next-to-leading order level, in *Proceedings, Ringberg Workshop on New Trends in HERA Physics 2005: Ringberg Castle, Tegernsee, Germany, October 2-7, 2005*, pp. 101–123, 2006, arXiv:hep-ph/0601021.
- [18] M. Dinsdale, M. Ternick, and S. Weinzierl, *Phys. Rev.* **D76**, 094003 (2007), arXiv:0709.1026.
- [19] S. Schumann and F. Krauss, *JHEP* **03**, 038 (2008), arXiv:0709.1027.
- [20] S. Plätzer and S. Gieseke, *Eur. Phys. J.* **C72**, 2187 (2012), arXiv:1109.6256.
- [21] Z. Nagy and D. E. Soper, *JHEP* **06**, 097 (2014), arXiv:1401.6364.
- [22] S. Höche and S. Prestel, *Eur. Phys. J.* **C75**, 461 (2015), arXiv:1506.05057.
- [23] M. Dasgupta, F. A. Dreyer, K. Hamilton, P. F. Monni, and G. P. Salam, *JHEP* **09**, 033 (2018), arXiv:1805.09327, [Erratum: *JHEP*03,083(2020)].
- [24] J. R. Forshaw, J. Holguin, and S. Plätzer, (2020), arXiv:2003.06400.
- [25] M. Dasgupta *et al.*, (2020), arXiv:2002.11114.
- [26] W. T. Giele, D. A. Kosower, and P. Z. Skands, *Phys. Rev.* **D78**, 014026 (2008), arXiv:0707.3652.
- [27] N. Fischer, S. Prestel, M. Ritzmann, and P. Skands, *Eur. Phys. J.* **C76**, 589 (2016), arXiv:1605.06142.
- [28] N. Fischer, A. Lifson, and P. Skands, *Eur. Phys. J.* **C77**, 719 (2017), arXiv:1708.01736.
- [29] A. H. Hoang, S. Plätzer, and D. Samitz, *JHEP* **10**, 200 (2018), arXiv:1807.06617.
- [30] A. H. Hoang and I. W. Stewart, *Nucl.Phys.Proc.Suppl.* **185**, 220 (2008), arXiv:0808.0222.
- [31] A. H. Hoang, The Top Mass: Interpretation and Theoretical Uncertainties, in *Proceedings, 7th International Workshop on Top Quark Physics (TOP2014): Cannes, France, September 28-October 3, 2014*, 2014, arXiv:1412.3649.

- [32] P. Nason, The Top Mass in Hadronic Collisions, in *From My Vast Repertoire ...: Guido Altarelli's Legacy*, edited by A. Levy, S. Forte, and G. Ridolfi, pp. 123–151, World Scientific, 2019, arXiv:1712.02796.
- [33] G. Corcella, R. Franceschini, and D. Kim, Nucl. Phys. **B929**, 485 (2018), arXiv:1712.05801.
- [34] G. Heinrich *et al.*, JHEP **07**, 129 (2018), arXiv:1709.08615.
- [35] S. Ferrario Ravasio, T. Ježo, P. Nason, and C. Oleari, Eur. Phys. J. **C78**, 458 (2018), arXiv:1801.03944.
- [36] A. H. Hoang, A. Jain, I. Scimemi, and I. W. Stewart, Phys.Rev.Lett. **101**, 151602 (2008), arXiv:0803.4214.
- [37] A. H. Hoang *et al.*, JHEP **04**, 003 (2018), arXiv:1704.01580.
- [38] S. Fleming, A. H. Hoang, S. Mantry, and I. W. Stewart, Phys.Rev. **D77**, 114003 (2008), arXiv:0711.2079.
- [39] G. Marchesini and B. Webber, Nucl. Phys. B **310**, 461 (1988).
- [40] S. Catani, B. Webber, and G. Marchesini, Nucl. Phys. B **349**, 635 (1991).
- [41] S. Brandt, C. Peyrou, R. Sosnowski, and A. Wroblewski, Phys. Lett. **12**, 57 (1964).
- [42] E. Farhi, Phys. Rev. Lett. **39**, 1587 (1977).
- [43] S. Fleming, A. H. Hoang, S. Mantry, and I. W. Stewart, Phys. Rev. **D77**, 074010 (2008), arXiv:hep-ph/0703207.
- [44] I. W. Stewart, F. J. Tackmann, and W. J. Waalewijn, Phys. Rev. Lett. **105**, 092002 (2010), arXiv:1004.2489.
- [45] Y. L. Dokshitzer and B. Webber, Phys. Lett. B **352**, 451 (1995), arXiv:hep-ph/9504219.
- [46] Y. L. Dokshitzer, G. Marchesini, and B. R. Webber, Nucl. Phys. **B469**, 93 (1996), hep-ph/9512336.
- [47] Y. L. Dokshitzer and B. R. Webber, Phys. Lett. **B404**, 321 (1997), hep-ph/9704298.
- [48] R. Abbate, M. Fickinger, A. H. Hoang, V. Mateu, and I. W. Stewart, Phys. Rev. **D83**, 074021 (2011), arXiv:1006.3080.
- [49] G. P. Korchemsky and G. F. Sterman, Nucl. Phys. B **555**, 335 (1999), arXiv:hep-ph/9902341.
- [50] G. Korchemsky and S. Tafat, JHEP **10**, 010 (2000), arXiv:hep-ph/0007005.
- [51] A. H. Hoang and I. W. Stewart, Phys. Lett. **B660**, 483 (2008), arXiv:0709.3519.